Rotational bands in ^{76}Rb

A. Harder, M.K. Kabadiyski,* K.P. Lieb, and D. Rudolph
II. Physikalisches Institut, Universität Göttingen, D-37073 Göttingen, Germany

C.J. Gross
Physics Division, Oak Ridge National Laboratory, Oak Ridge, Tennessee 37831-6371

R.A. Cunningham, F. Hannachi,† J. Simpson, and D.D. Warner
DRAL Daresbury Laboratory, Warrington WA4 4AD, United Kingdom

H.A. Roth and Ö. Skeppstedt
Department of Physics, Chalmers University of Technology, S-41296 Göteborg, Sweden

W. Gelletly
Physics Department, University of Surrey, Guildford GU2 5XH, United Kingdom

B.J. Varley
Schuster Laboratory, University of Manchester, Manchester M13 9PL, United Kingdom
(Received 15 February 1995)

High spin states in ^{76}Rb were investigated via the reaction ^{40}Ca(^{40}Ca,3pn)^{76}Rb at 128 MeV. The level scheme was established from $\gamma\gamma$, $\gamma\gamma\gamma$ and recoil-γ coincidences measured in the EUROGAM I array in combination with the Daresbury recoil separator. The known rotational bands were extended up to the excitation energy $E_x \approx 9.2$ MeV and spins $I^\pi = (21^+)$ and (19^-). The band head energies could be fixed by many interband transitions. Two new bands were identified. The level scheme is discussed in terms of the cranked shell model. In the negative parity bands ^{76}Rb behaves like a rigid rotor until the first band crossings.

PACS number(s): 21.10.Re, 23.20.Lv, 21.60.Ev, 27.50.+e

I. INTRODUCTION

The nuclei in the neutron-deficient $N = Z$ region around ^{76}Sr are expected to show large ground state deformations, due to the stabilizing effect of the pronounced deformed shell gap at nucleon number 38 in the single-particle spectrum [1]. For instance, in the neighboring nuclei experimental evidence was found for a large deformation up to $|\beta_2| \approx 0.4$ by means of lifetime measurements in ^{77}Rb [2] and laser spectroscopy in ^{77}Sr [3]. The latter study even identified the deformation as prolate. Thus, nuclei in this mass region are promising subjects of high-spin studies: Their excitation schemes are characterized by rotational bands of an extreme regularity. Recently, Gross *et al.* [4] found identical bands in ^{77}Sr, ^{78}Sr, and ^{78}Rb. The authors regarded them as evidence for the $[301]\frac{3}{2}$ orbital playing the role of a very good spectator.

In the present study we report on the investigation of the high-spin states of the $Z = 37, N = 39$ nucleus ^{76}Rb. Some information concerning this nucleus at low excitation energy was already known: The ground state spin $1^{(-)}$ had been determined by β radiation detected optical pumping (β-RADOP) [5] and conventional β-decay studies [6,7]. Hofmann *et al.* [8] had identified a 3.2 μs isomer to which they assigned $I^\pi = (4^+)$ from a comparison with the neighboring ^{74,76}Br nuclei. In a first high-spin study García Bermúdez *et al.* [9] established three strongly coupled rotational bands, reaching up to excitation energies $E_x \approx 2$ MeV and spins $I^\pi = 7^{(-)}$ and (10^+). In addition to bands built on the ground state and on the isomer they identified a third band, but its relative energy position could not be fixed. McNeill *et al.* [10] later confirmed these results, adding some transitions at the top of the known bands.

In this mass region neutron evaporation channels are very weak compared with charged particle evaporation in compound nucleus reactions and so the very efficient γ-ray spectrometer EUROGAM I was used [11–13] in combination with the Daresbury recoil separator [14] to try to extend our knowledge of the level schemes of ^{76}Rb and other nuclei near the $N = Z$ line in this mass region. Section II presents the experimental procedure and data evaluation. In Sec. III the results are summarized and in Sec. IV the level scheme is compared with those of neigh-

*Present address: Institut für Kernphysik, Universität zu Köln, D-50937 Köln, Germany.
†Present address: Centre de Spectrometrie Nucleaire et du Spectrometrie de Masse, IN2P3-CNRS, Orsay, France.

boring nuclei and interpreted in terms of the cranked shell model.

II. EXPERIMENT AND DATA REDUCTION

In the experiment the ^{40}Ca(^{40}Ca,3pn) reaction was studied at 128 MeV bombarding energy because it is expected to populate high-spin states in ^{76}Rb. The resulting γ radiation was detected with the EUROGAM I array which was coupled to the Daresbury recoil separator. EUROGAM I contained 45 Compton-suppressed Ge detectors at 72° (10 detectors), 86° (5), 94° (5), 108° (10), 134° (10), and 158° (5). The target consisted of 250 μg/cm^2 of ^{40}Ca, enriched to 99.965%, which had been evaporated onto a 10 μg/cm^2 carbon foil and covered with a flash of gold to prevent oxidation. It was mounted with the carbon side facing the recoil separator. Radioactive sources of ^{152}Eu, ^{133}Ba and (for high γ-ray energies) ^{88}Y were used for energy and efficiency calibration.

With the recoil separator allowing the identification of A and Z of the recoiling nuclei, recoil-γ coincidence events as well as twofold and higher γ coincidences were recorded. The reaction channel of interest leading to ^{76}Rb is populated with a relative cross section of only some 3% of the fusion cross section, as opposed to the strong, purely charged particle reaction channels like ^{77}Rb + 3p, ^{76}Kr + 4p, and ^{74}Kr + α2p which sum to a total of 94%. Thus, the $\gamma\gamma$ coincidence spectra are dominated by events from the latter nuclei. As a result it is difficult to obtain uncontaminated spectra for ^{76}Rb, especially in the case of the stretched $E2$ transitions at higher energies. Resolving the lines becomes even more difficult because of the Doppler broadening due to the recoiling nuclei. However, the strongly coupled bands identified previously in ^{76}Rb contained a number of strong transitions at low energies (e.g., 101, 180, 242 keV), which could be used as gates. A total of 2.3 × 10^8 triple-γ events for all reactions were collected, from which new and unambiguous information about the high-spin level scheme of ^{76}Rb was obtained: For each of the three previously known bands a two-dimensional $\gamma\gamma$ matrix was sorted, by imposing the additional condition that the double event be in coincidence with a third low-lying γ transition in the corresponding band. For this purpose the 180, 210, 390, 550, and 643 keV transitions in band 1, the 101, 208, 321, and 444 keV transitions in band 3, and the 104, 242, 291, and 333 keV transitions in band 4 were used. The band identification numbers refer to the labels in Table I (and Fig. 2). This procedure resulted in clean "one-band" ^{76}Rb matrices and triples coincidence spectra, examples of which are shown in Fig. 1. Each spectrum shown represents the sum of several gates and clearly displays all the transitions in the respective band without any contamination from the other strong

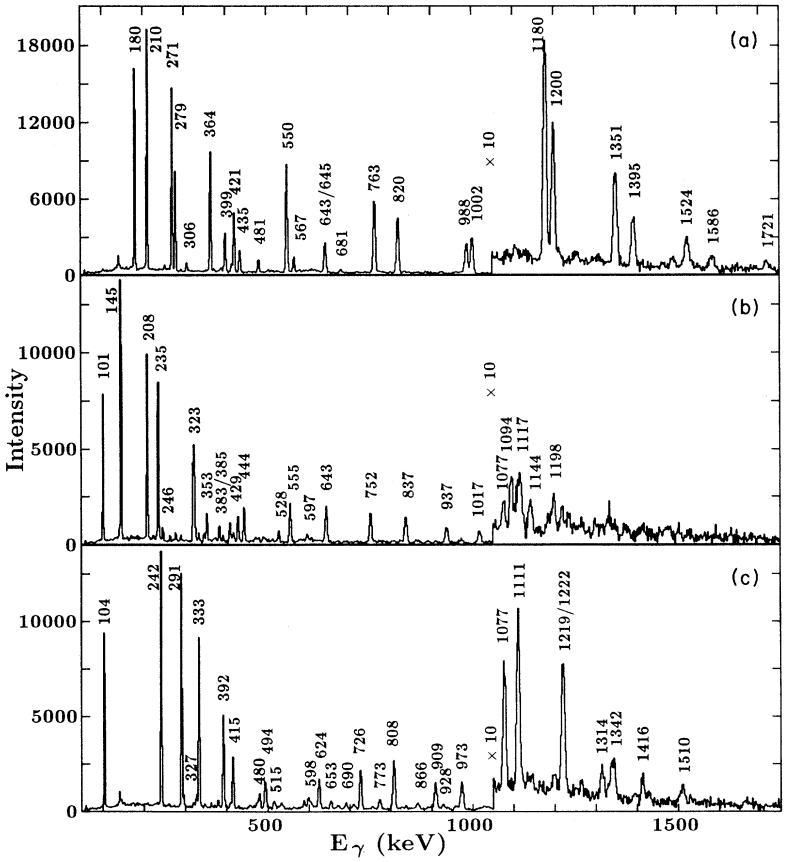

FIG. 1. Triple-γ coincidence spectra of ^{76}Rb. The energy labels are in keV. (a) Sum of the spectra in coincidence with the 180, 210, 271, 279, 364, and 550 keV transitions in the matrix for band 1. (b) Sum of the spectra in coincidence with the 101, 145, 208, 235, 321, and 323 keV transitions in the matrix for band 3. (c) Sum of the spectra in coincidence with the 104, 242, 291, and 333 keV transitions in the matrix for band 4.

TABLE I. Excitation energies, transition energies, DCO ratios, and spin assignments.

E_x (keV)	E_γ (keV)	$I_{\rm rel}$ at 64°	$R_{\rm DCO}$	Gate[a]	Multipolarity	I_i^π ($\hbar$)	I_f^π ($\hbar$)
			Band 1				
317.4(2)	70.6(1)[c]				$(E1)$	$4^{(+)}$	$3^{(-)}$
497.5(2)	180.2(1)	100(4)	0.94(2)	D	$E2/M1$	$5^{(+)}$	$4^{(+)}$
707.6(3)	210.1(1)	100(11)	1.10(2)	C	$E2/M1$	$6^{(+)}$	$5^{(+)}$
	390.1(2)	50(3)			$E2$	$6^{(+)}$	$4^{(+)}$
978.3(3)	270.7(1)	47(3)	1.13(4)	D	$E2/M1$	$7^{(+)}$	$6^{(+)}$
	480.7(2)	44(5)	0.63(3)	C	$E2$	$7^{(+)}$	$5^{(+)}$
1257.1(3)	278.8(1)	29(3)	1.16(7)	D	$E2/M1$	$8^{(+)}$	$7^{(+)}$
	549.6(1)	81(5)	0.44(2)	CD	$E2$	$8^{(+)}$	$6^{(+)}$
1621.2(3)	364.1(1)	34(4)	1.40(8)	D	$E2/M1$	$9^{(+)}$	$8^{(+)}$
	642.8(3)	49(5)	[b]		$E2$	$9^{(+)}$	$7^{(+)}$
2020.3(3)	399.1(1)	11(1)	1.51(18)	D	$E2/M1$	$10^{(+)}$	$9^{(+)}$
	763.3(3)	60(4)	0.42(2)	CD	$E2$	$10^{(+)}$	$8^{(+)}$
2441.4(3)	421.3(1)	24(3)	1.11(9)	D	$E2/M1$	$11^{(+)}$	$10^{(+)}$
	820.1(1)	66(9)	0.38(2)	CD	$E2$	$11^{(+)}$	$9^{(+)}$
3008.1(3)	566.8(2)	8(1)			$E2/M1$	$12^{(+)}$	$11^{(+)}$
	987.7(2)	35(2)	0.43(2)	CD	$E2$	$12^{(+)}$	$10^{(+)}$
3442.9(3)	434.8(2)	9(1)			$E2/M1$	$13^{(+)}$	$12^{(+)}$
	1001.5(3)	46(5)	0.46(2)	CD	$E2$	$13^{(+)}$	$11^{(+)}$
4207.9(4)	765.4(5)	4(1)			$E2/M1$	$14^{(+)}$	$13^{(+)}$
	1199.5(4)	23(2)	0.41(3)	CD	$E2$	$14^{(+)}$	$12^{(+)}$
4623.1(4)	415.2(3)	3(1)			$E2/M1$	$15^{(+)}$	$14^{(+)}$
	1180.2(4)	40(4)	0.35(2)	CD	$E2$	$15^{(+)}$	$13^{(+)}$
5602(1)	1394.6(10)	11(1)	0.52(4)	CD	$E2$	$16^{(+)}$	$14^{(+)}$
5973.6(7)	1350.5(5)	22(2)	0.51(3)	CD	$E2$	$17^{(+)}$	$15^{(+)}$
7188(1)	1586(1)	9(1)	0.43(5)	CD	$E2$	$18^{(+)}$	$16^{(+)}$
7497.5(8)	1524(1)	7(1)	0.31(5)	CD	$E2$	$19^{(+)}$	$17^{(+)}$
9218(1)	1721(1)	2(1)			$(E2)$	(21^+)	$19^{(+)}$
			Band 2				
629.3(5)	132(1)	3(1)	[b]			(4)	$5^{(+)}$
	312(1)	9(1)				(4)	$4^{(+)}$
	383(2)	7(4)	[b]			(4)	$3^{(-)}$
1013.7(3)	306.1(2)	4(1)	0.59(6)	CD	$(\Delta I = 0)$	(6)	$6^{(+)}$
	324(1)	1(1)	[b]		$(\Delta I = 1)$	(6)	$5^{(-)}$
	384.5(7)	20(5)	0.61(12)	C	$(E2)$	(6)	(4)
1525.4(5)	511.8(6)	8(3)					(6)
1659.1(4)	133.7(5)	2(1)	[b]			(8)	
	645.2(5)	16(8)	[b]		$(E2)$	(8)	(6)
	680.9(4)	4(1)	> 1	C	$(\Delta I = 1)$	(8)	$7^{(+)}$
2548.4(9)	889.3(8)	5(2)	0.64(10)	C	$E2$	(10)	(8)
3656(2)	1108(2)	3(1)	0.55(9)	C	$E2$	(12)	(10)
4963(3)	1307(2)	2(1)	$\ll 1$	C	$(E2)$	(14)	(12)
			Band 3				
101.2(1)	101.2(1)	12(1)	0.97(5)	B	$E2/M1$	$2^{(-)}$	$1^{(-)}$
246.3(1)	145.1(1)	25(2)	0.97(3)	A	$E2/M1$	$3^{(-)}$	$2^{(-)}$
	246.4(2)	13(1)	0.60(9)	A	$E2$	$3^{(-)}$	$1^{(-)}$
454.7(1)	208.4(1)	35(5)	1.02(5)	A	$E2/M1$	$4^{(-)}$	$3^{(-)}$
	353.4(3)	26(2)	0.89(8)	A	$E2$	$4^{(-)}$	$2^{(-)}$
689.8(1)	235.1(1)	23(2)	1.17(7)	A	$E2/M1$	$5^{(-)}$	$4^{(-)}$
	269(2)	1(1)			$E2/M1$	$5^{(-)}$	$4^{(-)}$
	443.5(1)	25(2)	0.56(5)	A	$E2$	$5^{(-)}$	$3^{(-)}$
1010.4(1)	320.5(1)	19(2)	1.29(10)	AB	$E2/M1$	$6^{(-)}$	$5^{(-)}$
	555.7(1)	26(3)	0.69(6)	A	$E2$	$6^{(-)}$	$4^{(-)}$
1333.3(2)	322.9(1)	17(2)	1.19(10)	AB	$E2/M1$	$7^{(-)}$	$6^{(-)}$
	379.1(5)	1(1)			$E2/M1$	$7^{(-)}$	$6^{(-)}$
	643.1(3)	30(5)	[b]			$7^{(-)}$	$5^{(-)}$

TABLE I. *(Continued).*

E_x (keV)	E_γ (keV)	I_{rel} at 64°	R_{DCO}	Gate[a]	Multipolarity	I_i^π ($\hbar$)	I_f^π ($\hbar$)
1761.7(2)	428.6(3)	7(1)			$E2/M1$	$8^{(-)}$	$7^{(-)}$
	751.6(3)	20(3)	0.53(5)	AB	$E2$	$8^{(-)}$	$6^{(-)}$
2170.7(2)	409.1(2)	8(1)			$E2/M1$	$9^{(-)}$	$8^{(-)}$
	490.3(10)	1(1)			$E2/M1$	$9^{(-)}$	$8^{(-)}$
	837.3(2)	20(3)	0.61(4)	AB	$E2$	$9^{(-)}$	$7^{(-)}$
2698.7(3)	527.5(3)	5(1)			$E2/M1$	$10^{(-)}$	$9^{(-)}$
	937.2(2)	14(2)	0.47(4)	AB	$E2$	$10^{(-)}$	$8^{(-)}$
2905(1)	1143.4(10)	3(1)					$8^{(-)}$
3187.7(4)	488.8(5)	2(1)			$E2/M1$	$11^{(-)}$	$10^{(-)}$
	1017.2(5)	12(2)	0.49(6)	AB	$E2$	$11^{(-)}$	$9^{(-)}$
3792.6(6)	1093.9(5)	4(1)	0.43(6)	AB	$E2$	$12^{(-)}$	$10^{(-)}$
4305(1)	1117(1)	6(1)			$(E2)$	(13^-)	$11^{(-)}$
5503(1)	1198(1)	4(1)			$(E2)$	(15^-)	(13^-)
			Band 4				
421.6(2)	104.2(1)	21(2)	0.73(3)	E	$\Delta I = 0$	$4^{(-)}$	$4^{(+)}$
	175.8(5)	1(1)			$E2/M1$	$4^{(-)}$	$3^{(-)}$
	320(1)	5(1)			$E2$	$4^{(-)}$	$2^{(-)}$
663.2(2)	208.4(2)	1(1)			$E2/M1$	$5^{(-)}$	$4^{(-)}$
	241.7(1)	63(4)	0.88(5)	F	$E2/M1$	$5^{(-)}$	$4^{(-)}$
954.1(2)	264.3(5)	2(1)			$E2/M1$	$6^{(-)}$	$5^{(-)}$
	290.9(1)	39(3)	1.38(8)	E	$E2/M1$	$6^{(-)}$	$5^{(-)}$
	532.4(5)	11(1)			$E2$	$6^{(-)}$	$4^{(-)}$
1287.5(2)	277.1(5)	2(1)			$E2/M1$	$7^{(-)}$	$6^{(-)}$
	333.4(1)	25(2)	1.09(7)	F	$E2/M1$	$7^{(-)}$	$6^{(-)}$
	597.7(5)	[b]			$E2$	$7^{(-)}$	$5^{(-)}$
	624.2(2)	27(4)	[b]		$E2$	$7^{(-)}$	$5^{(-)}$
1679.7(2)	346.2(5)	2(1)			$E2/M1$	$8^{(-)}$	$7^{(-)}$
	392.3(1)	13(1)	1.24(9)	EF	$E2/M1$	$8^{(-)}$	$7^{(-)}$
	725.6(1)	13(1)	0.36(3)	EF	$E2$	$8^{(-)}$	$6^{(-)}$
2095.1(2)	415.3(2)	8(1)	1.17(10)	EF	$E2/M1$	$9^{(-)}$	$8^{(-)}$
	807.5(2)	17(2)	0.35(3)	EF	$E2$	$9^{(-)}$	$7^{(-)}$
2589.0(2)	418.6(5)	3(1)			$E2/M1$	$10^{(-)}$	$9^{(-)}$
	493.5(3)	8(1)			$E2/M1$	$10^{(-)}$	$9^{(-)}$
	909.3(1)	13(1)	0.60(7)	EF	$E2$	$10^{(-)}$	$8^{(-)}$
3068.4(3)	479.7(3)	4(1)			$E2/M1$	$11^{(-)}$	$10^{(-)}$
	973.2(2)	18(3)	0.41(5)	EF	$E2$	$11^{(-)}$	$9^{(-)}$
3666.1(3)	598.2(5)	1(1)			$E2/M1$	$12^{(-)}$	$11^{(-)}$
	1077.0(3)	7(1)	$\ll 1$	EF	$(E2)$	$12^{(-)}$	$10^{(-)}$
4180.2(4)	514.6(5)	1(1)			$(E2/M1)$	$13^{(-)}$	$12^{(-)}$
	1111.4(5)	13(2)	$\ll 1$	EF	$(E2)$	$13^{(-)}$	$11^{(-)}$
4885(1)	1219(1)	4(2)	[b]		$(E2)$	(14^-)	$12^{(-)}$
5402(1)	1222(1)	6(2)	[b]		$(E2)$	(15^-)	$13^{(-)}$
6199(1)	1314(1)	2(1)			$(E2)$	(16^-)	(14^-)
6744(1)	1342(1)	4(1)			$(E2)$	(17^-)	(15^-)
7615(2)	1416(1)	1(1)			$(E2)$	(18^-)	(16^-)
8254(2)	1510(1)	2(1)			$(E2)$	(19^-)	(17^-)
			Band 5				
692(1)	271(2)	1(1)					$4^{(-)}$
990.1(9)	296(2)	1(1)					
	568(2)	2(1)					$4^{(-)}$
1250.3(3)	260(1)	1(1)				6	
	296.2(5)	1(1)			$\Delta I = 0$	6	$6^{(-)}$
	587.4(4)	6(1)	1.00(20)	E	$\Delta I = 1$	6	$5^{(-)}$
1577.4(3)	327.1(2)	5(1)			$(E2/M1)$	(7)	6
	623.1(5)	4(1)	[b]		$(\Delta I = 1)$	(7)	$6^{(-)}$

TABLE I. *(Continued).*

E_x (keV)	E_γ (keV)	$I_{\rm rel}$ at 64°	$R_{\rm DCO}$	Gate[a]	Multipolarity	I_i^π ($\hbar$)	I_f^π ($\hbar$)
1940.3(3)	362.8(3)	3(1)			$(E2/M1)$	(8)	(7)
	652.6(5)	2(1)			$(\Delta I = 1)$	(8)	$7^{(-)}$
	690.0(3)	5(1)			$(E2)$	(8)	6
2350.3(5)	409(1)	2(1)			$(E2/M1)$	(9)	(8)
	671(1)	1(1)			$(\Delta I = 1)$	(9)	$8^{(-)}$
	773.0(5)	9(1)			$(E2)$	(9)	(7)
2806.0(4)	455(1)	1(1)			$(E2/M1)$	(10)	(9)
	710(1)	3(1)			$(\Delta I = 1)$	(10)	$9^{(-)}$
	865.8(3)	7(1)			$(E2)$	(10)	(8)
3278.3(7)	928.0(5)	5(1)			$(E2)$	(11)	(9)
3846(2)	1040(2)	4(1)			$(E2)$	(12)	(10)
4307(2)	1029(1)	3(1)			$(E2)$	(13)	(11)

[a] A, 101 keV; B, 208 keV; C, 180 keV; D, 210 keV; E, 242 keV; F, 291 keV.
[b] Doublet structure.
[c] From Ref. [8].

reaction channels. When evaluating these data, gates could be set not only on low energy transitions but also on the transitions on top of the bands, thereby confirming their placement and helping to construct a consistent level scheme. All transitions identified in ^{76}Rb from the recoil-γ coincidence data have been placed in the level scheme.

The geometry of the EUROGAM I setup also allowed the assignment of spins from the angular correlations of the γ rays. For this purpose, a matrix was constructed in which γ events recorded at 158° were sorted against those recorded at 86° and 94°. Selecting energies on both axes yielded directional correlations of oriented states (DCO ratios), here defined as

$$R_{\rm DCO} := \frac{I(\gamma_1 \text{ at } 86°, 94°; \text{gated with } \gamma_2 \text{ at } 158°)}{I(\gamma_1 \text{ at } 158°; \text{gated with } \gamma_2 \text{ at } 86°, 94°)}, \quad (1)$$

with the gate (γ_2) set on an $M1$ transition. The usual way of gating on stretched $E2$ transitions was not feasible due to the low intensity of these transitions or too strong contaminations. The DCO ratios were not corrected for detection efficiency because the relative efficiency of the five detectors in the 158° ring was found to be equal to that of the ten detectors at 86° and 94° within the 3% accuracy of the efficiency calibration. These DCO ratios were evaluated to obtain information about the multipole character of the transitions; some 50 DCO ratios could be deduced. They are given in Table I together with the corresponding gates. In some cases two gates were summed up in order to improve the statistics. This procedure does not significantly affect the resulting DCO ratio as shown in a recent work of Kabadiyski *et al.* [15]. The expected values are $R_{\rm DCO} = 1$ for a stretched pure dipole transition, $R_{\rm DCO} \approx 0.5$ for a stretched $E2$ transition, and $R_{\rm DCO} \approx 0.4$ for pure dipole $\Delta I = 0$ transitions. These values were calculated for cascades of three or four members and a variable number of dipole and quadrupole intermediate transitions. A pure $M1$ gate and an average initial alignment of the cascade of $\alpha_2 = 0.85$ were assumed.

III. RESULTS

All of the information now available on high-spin states in ^{76}Rb is summarized in Table I. The resulting level scheme shown in Fig. 2 comprises more than 60 states, which are connected by some 120 transitions and can be grouped into 5 rotational bands. The present work confirms the previous studies, which reached up to $E_x \approx 6$ MeV [10] ($E_x \approx 2$ MeV [9]); the only exception is the 1117 keV transition in band 3, which is placed in the other signature component compared to the suggestion in [10]. The previously known bands (labeled 1, 3, and 4 in Fig. 2 and Table I) were extended to excitation energies $E_x = 9.2$ MeV and spins $I^\pi = (21^+)$ for positive parity and to $E_x = 8.3$ MeV and $I^\pi = (19^-)$ for negative parity states. The spin assignments were made according to the following criteria.

(a) DCO ratios — a DCO ratio must be consistent with only one of the values given in Sec. II above.

(b) Summed energy — if two subsequent in-band transitions and a crossover transition lead to the same final state, the crossover transition is of $E2$ character and the two are mixed $E2/M1$ transitions.

(c) The assumption is made that γ-ray multipolarities are either dipoles or of $E2$ character.

(d) In view of the rotorlike patterns of the observed cascades, the systematics of transition energies may be used to make probable spin-parity assignments for the weakly populated states.

(e) Finally yrast arguments are assumed for the spin assignments. All assignments are based on the previous results for the ground state and the isomeric state spin [5–7].

The main decay path through the nucleus was found

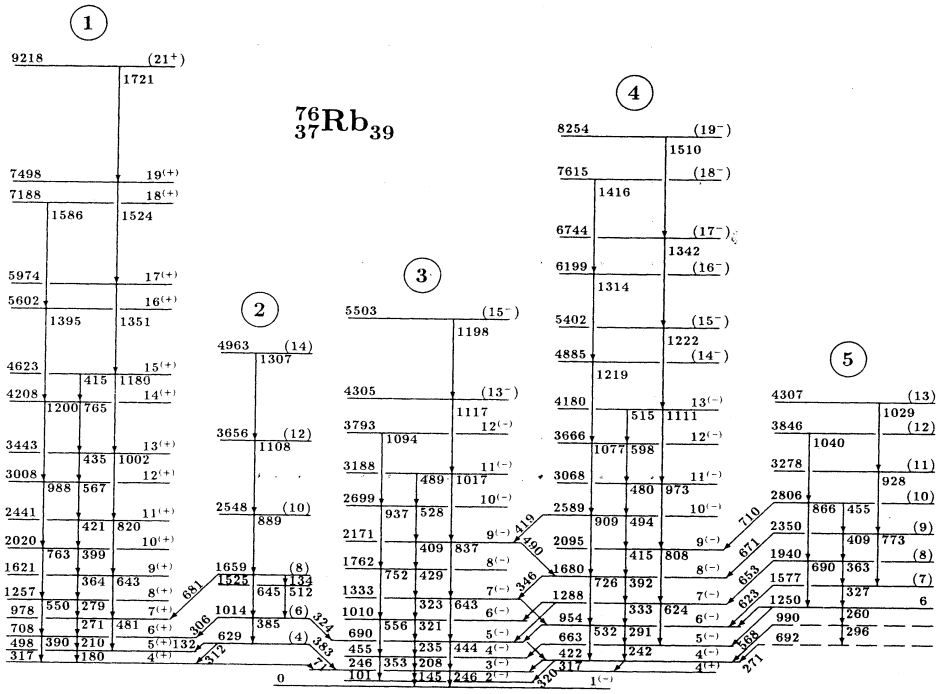

FIG. 2. Proposed level scheme of ^{76}Rb. Five rotational bands, connected by some 25 interband transitions, have been established. The energy labels of some interband transitions have been omitted for the sake of legibility. See Table I for more information.

to pass through band 1, which is consistent with the previous observations. Accordingly all of the γ-ray relative intensities were normalized to that of the 180 keV transition: $I_{\rm rel}(180\ {\rm keV}) = 100(4)$. The normalization to the other bands was done with the ^{76}Rb recoil-γ spectrum. The missing intensities of some depopulating transitions of some low-lying states are due to their presumed long lifetimes.

The positive parity yrast states, band 1, are established up to 9218 keV and spin $I^\pi = (21^+)$. The bandhead is the $4^{(+)}$ 317 keV, isomeric (3.2 μs) state identified by Hofmann *et al.* [8]. DCO ratios could be deduced for most of the $E2$ transitions as well as for the first seven $M1$ transitions. Therefore definite spins could be assigned to all but the highest level in band 1. For the highest state observed the spin assignment $I^\pi = (21^+)$ follows from the $I(I+1)$ structure of the band. $M1$ transitions connecting the signature partners are observed up to $I^\pi = 15^{(+)}$. A significant signature splitting was observed in this band.

Several new lines, e.g., at 306 and 681 keV, were identified to be in coincidence with the low-lying transitions in band 1 (see Fig. 1). These γ rays were found to depopulate a new rotational band, labeled band 2. Four interband transitions connect it with band 1, fixing the relative excitation energy of band 2. From the measured DCO ratios the $E2$ character could be assigned to the transitions within this band. The 681 keV γ ray leading to band 1 was identified to be a dipole transition. Hence, the level spins of this band could be fixed, reaching up to $I = (14)$. The DCO ratio of the 306 keV interband transition is consistent with $\Delta I = 0$ and confirms the $I = 6$ assignment.

Band 3 is built upon the $1^{(-)}$ ground state. It was extended to the excitation energy $E_x = 5503$ keV. Within this band, it was possible to deduce spins from DCO ratios for levels up to the $12^{(-)}$ state. The spins of the remaining two states lying above the $12^{(-)}$ state were tentatively assigned on the assumption that the regular increase in the transition energies is consistent with the rotational pattern.

Gates on some of the low-lying transitions also displayed lines belonging to band 2 and two further interband transitions, this time between bands 2 and 3, thus confirming the previously established energy position of band 2, and are consistent with its spin assignments. Furthermore, an 1143 keV transition was observed to feed the $8^{(-)}$ 1762 keV state from outside the band.

The lowest transitions of band 4 had been identified by García Bermúdez *et al.* [9], but they were unable to pin down the relative bandhead energy. In the present study the band was not only extended to much higher energies ($E_x = 8254$ keV), but its bandhead energy could be determined on the basis of the many interband transitions observed between bands 3 and 4. Apart from the 104 keV transition from the lowest level no connection with the positive parity band 1 was found. The bandhead spin was deduced from the DCO ratio of the 104 keV transition, which connects the bandhead with the $4^{(+)}$, 317 keV isomeric state [8], and from systematics: On the assumption that only dipole or $E2$ transitions are observed, the interband transitions between band 3 and band 4 limit the possible spin assignments of the 422 keV state to $I^\pi = 3^{(-)},4^{(-)}$. The DCO ratio of the 104 keV transition excludes a $\Delta I = 1$ transition, leaving the possibilities of $\Delta I = 0,2$. The latter is thus eliminated because it would mean an $M2$ transition. In addition, an $M2$ transition of this energy would be highly converted and the 422 keV state would be isomeric. This

leads to a bandhead spin of $I^\pi = 4^{(-)}$. On the assumption that the ground state is of negative parity, band 4 is the negative parity yrast band starting with the $4^{(-)}$ bandhead, in agreement with the fact that it can be observed up to significantly higher energies (8254 keV) and spins (19^-) than the same parity band 3. This band is weaker than the positive parity yrast band and DCO ratios could be obtained only for transitions from states up to $I^\pi = 13^{(-)}$. The spin assignments of the higher states are again based on the regular increase of the transition energies.

As in the case of the "band 1" and "band 3" matrices, gating on low-lying transitions in the "band 4" matrix revealed a number of transitions previously unknown which form into an additional rotational band, labeled band 5 in Fig. 2. Several states of this new band decay into band 4, definitely fixing its energy position. This band also follows a distinct $E_x \sim I(I+1)$ dependence, which was adapted as the basis for the spin assignments within this band. The DCO ratio of the 587 keV transition, which connects the 1250 keV level with the $5^{(-)}$, 663 keV level of band 4, fixes the spins of band 5. Below the $I = 6$, 1250 keV state, some quite weak depopulating transitions to the head of band 4 are proposed. The $I = (13)$, 4307 keV level at the top of band 5 is within 2 keV of the $I^\pi = (13^-)$ state of band 3. However, in the triple-γ event matrices a coincidence between the 1029 keV (band 5) and the 1198 keV (band 3) could be proved neither wrong nor true due to poor statistics. The corresponding $\gamma\gamma$ coincidence spectra failed to give proof as well because of too many strong contaminations from other reaction channels.

IV. DISCUSSION

All the bands in ^{76}Rb show a rather regular $E_x \sim I(I+1)$ dependence, which is a property of rotational excitation. Consequently, it makes sense to examine their kinematical ($\mathcal{J}^{(1)}$) and dynamical ($\mathcal{J}^{(2)}$) moments of inertia. In Fig. 3 they are presented as a function of rotational frequency ($\hbar\omega$). Also plotted is the alignment i of the bands [16]. The alignment is plotted relative to the ground state band in ^{78}Sr [17] using the Harris parameters ($18\,\hbar$/MeV,0,0) [18].

García Bermúdez *et al.* [9] reported a constant kinematical moment of inertia for band 3 up to spin $7^{(-)}$. In the present work this can be extended up to $I = (15^-)$: Both the kinematical and the dynamical moments of inertia are similar and rather constant until $\hbar\omega = 0.6$ MeV, indicating rigid rotation in this band. Then the sharp increase marks a band crossing. The value of $\mathcal{J}^{(1)} \approx \mathcal{J}^{(2)} \approx 20\,\hbar^2$/MeV corresponds to those in the neighboring nuclei and leads us to suggest a ground state configuration composed of the odd proton ($Z = 37$) occupying the $[312]\frac{3}{2}^-$ and the odd neutron ($N = 39$) the $[422]\frac{5}{2}^+$ orbital at prolate deformation $\beta_2 \approx 0.4$ in the Nilsson scheme. The corresponding part of the single-particle spectrum is shown in Fig. 4. This combination is consistent with the observed ground state spins in ^{77}Rb [19] and ^{77}Sr [3,20], as adding a second neutron or proton

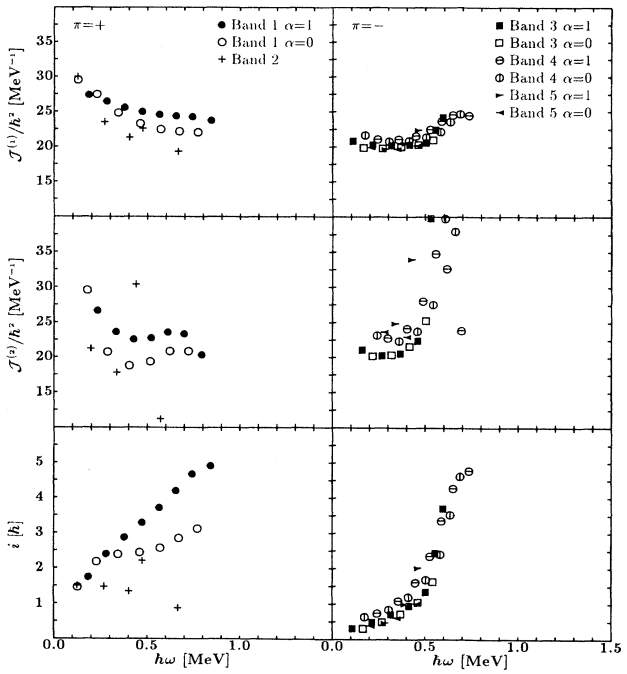

FIG. 3. Kinematical ($\mathcal{J}^{(1)}$) and dynamical ($\mathcal{J}^{(2)}$) moments of inertia and alignment i of the positive parity (left hand side) and negative parity (right hand side) bands of ^{76}Rb.

to the respective unpaired nucleon results in $I^\pi = \frac{3}{2}^-$ in ^{77}Rb and $\frac{5}{2}^+$ in ^{77}Sr.

Figure 5 compares the moments of inertia $\mathcal{J}^{(1)}$ and $\mathcal{J}^{(2)}$ and the alignments i of the ground state bands in ^{77}Sr, ^{77}Rb, and ^{76}Rb and reveals a striking similarity in their behavior: Their moments of inertia, especially the dynamical ones, hardly differ. In the case of ^{77}Rb and ^{77}Sr this can be observed even beyond the band crossing, which occurs at about the same frequency $\hbar\omega \approx 0.6$ MeV in all three nuclei. The band crossings are accompanied by a large gain ($\Delta i \approx 5\hbar$) in alignment, which is inter-

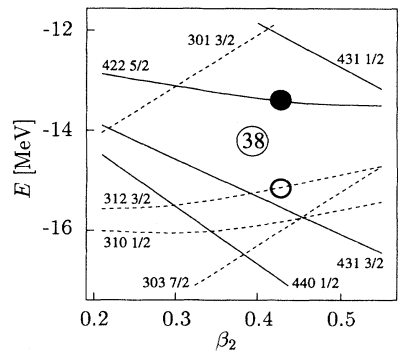

FIG. 4. Proposed configuration of the $1^{(-)}$ ground state of ^{76}Rb in the single-particle spectrum calculated by Nazarewicz *et al.* [1]. The solid circle (•) symbolizes the odd neutron ($N = 39$), the empty circle (○) the odd proton ($Z = 37$).

preted as the breaking of a $g_{\frac{9}{2}}$ proton pair. In ^{76}Rb and ^{77}Sr the unpaired neutron in the $[422]\frac{5}{2}$ orbital blocks the alignment of a neutron pair. Hence this is most probably a proton band crossing, in accordance with the observations in ^{78}Sr, where the first crossing was found to occur at $\hbar\omega \approx 0.6$ MeV [17].

More than ten transitions connect band 3 and band 4, which is an indication of similar band structures. Furthermore, the moments of inertia do not differ significantly, although the characteristic of $\mathcal{J}^{(1)} = \mathcal{J}^{(2)}$ of rigid rotation in band 4 is not as well fulfilled as in the ground band. An upbending is noted at about the same rotational frequency as in band 3. Here a plausible configuration is given by the excitation of a proton from the $[310]\frac{1}{2}^-$ orbital to the $[312]\frac{3}{2}^-$ orbital. This yields a bandhead spin of $I^\pi = 3^-$ in agreement with the value determined experimentally. The predicted energy difference for the above Nilsson orbitals [1] amounts to approximately 0.5 MeV; in the level scheme the bandhead was fixed (see above) at a comparable value of 422 keV. However, another possibility is an identical configuration as that of the ground state with the spins coupling parallel instead of antiparallel.

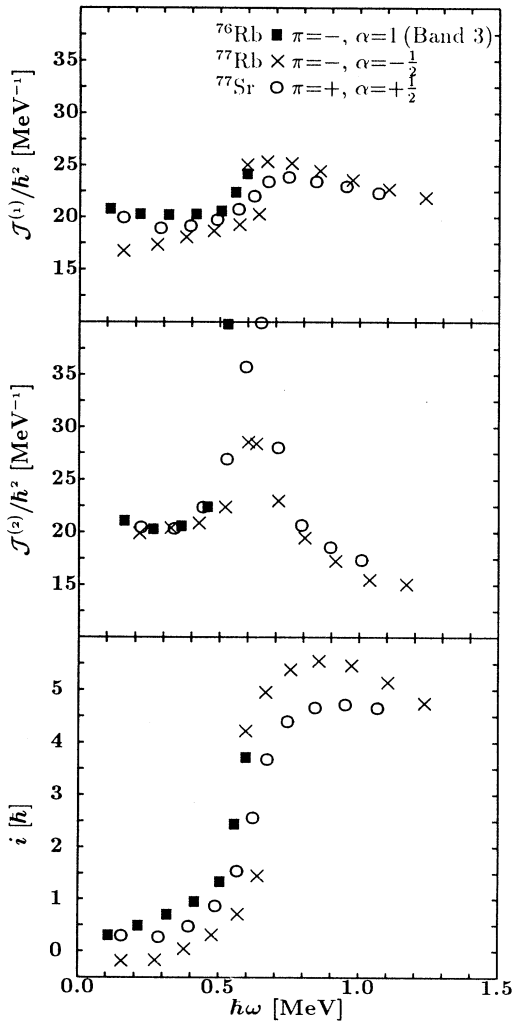

FIG. 5. Comparison of the kinematical ($\mathcal{J}^{(1)}$) and dynamical ($\mathcal{J}^{(2)}$) moments of inertia and the alignment i of the ground state bands in ^{76}Rb, ^{77}Rb, and ^{77}Sr.

Many states in band 5 also decay to band 4, so that again a similarity in the structure of both bands is evident. In contrast to band 4 we suggest that a proton from the $[303]\ \frac{7}{2}^-$ orbital is excited to the $[312]\frac{3}{2}^-$ orbital at about the same deformation as in bands 3 and 4. This would give negative parity to this band and a bandhead spin of $I^\pi = 6^-$, in agreement with the experimental value for the 1250 keV state, which we interpret as the head of this band. The predicted energy gap of ≈ 1 MeV between the above orbitals is consistent with the observed excitation energy. Although only a few transitions are available, the moments of inertia we deduce fit well into the scheme set by the negative parity bands 3 and 4 (Fig. 3).

The positive parity band 1 shows a different behavior. Starting from the values $\mathcal{J}^{(1)} \approx \mathcal{J}^{(2)} \approx 30\,\hbar^2/\text{MeV}$, the moments of inertia decrease at higher rotational frequencies. The configuration of the bandhead can be described by a $\pi[431]\frac{3}{2}^+, \nu[422]\frac{5}{2}^+$ Nilsson configuration, which would be accompanied by a slight decrease in deformation. This observation agrees with the suggestion of Hofmann *et al.* [8] who concluded, from the strongly reduced transition probability (3×10^{-7} W.u.) of the 71 keV transition, that these bands possess different core particle structures possibly connected with shape coexistence. The fact that no other crossover transitions were observed between bands 1 and 3 makes this argument even more plausible. Lifetime measurements in these bands will allow the deduction of quadrupole moments, supplying information about the respective deformations.

Although the transition energies provide a clear rotational structure as in all the other bands, a distinct signature splitting is apparent, and the assumed $(\pi g_{\frac{9}{2}}, \nu g_{\frac{9}{2}})$ configuration would account for it. Besides no band crossing would be expected as both the proton and the neutron alignment are blocked in this case, and in fact none is observed. In order to illustrate the signature splitting, the quantity $[E(I) - E(I-1)]/2I$ is plotted versus I in Fig. 6. A weak alternating pattern can be observed at low excitation spins which becomes much more distinct above $I = 9\,\hbar$. This increase is accompanied by a phase reversal in the alternating staggering, i.e., a change in the sign of the signature splitting. This feature has already been identified before in the positive parity band of the isotone ^{74}Br [21] and also occurs in the isotope ^{78}Rb [10] in the band built on the $I = 4$ isomer. Graphs of these bands are included in Fig. 6 for comparison. This feature has been predicted by Kreiner and Mariscotti [22] based upon calculations in a two noninteracting quasiparticles plus rotor model. The signature inversion takes place at spin $I = 9\,\hbar$ because it represents the highest value based on the intrinsic motion of two $g_{\frac{9}{2}}$ nucleons. Below this spin states are mainly built by a combination of collective rotation and realignment of the intrinsic spins whereas above $9\,\hbar$ rotation of a system with two fully

aligned quasiparticles is involved. This change in structure leads to the observed signature inversion.

In band 2, the signature splitting seems to be even more pronounced since only $\alpha = 0$ states are observed. The 1525 keV state might be the single representative of the unfavored signature states. The low-lying levels of band 2 decay to both bands 1 and 3 with similar strengths. This suggests a structure which might serve as a "bridge" between the otherwise noncommunicating bands.

The moments of inertia of the second band show a similar behavior to that of band 1: Starting from a high value of $\mathcal{J}^{(1)} \approx 30\ \hbar^2/\mathrm{MeV}$ they decrease as the rotational frequency grows larger.

In Fig. 7, $\mathcal{J}^{(1)}$, $\mathcal{J}^{(2)}$, and i of band 1 are compared with a strongly coupled band in ^{77}Rb, recently identified in the course of this experiment [23]. It is suggested that it is built upon a $\pi[431]\frac{3}{2}^+ \times \nu[422]\frac{5}{2}^+ \times \nu[301]\frac{3}{2}^-$ configuration; i.e., it only differs from the proposed configuration of band 1 by an additional neutron in the $[301]\frac{3}{2}^-$ orbital. Again, remarkable similarities can be observed: The kinematical moments of inertia start at the same value and decrease with the same slope, the dynamical moments of inertia behave similarly, and, finally, the alignments in both bands show the same steady increase without a clear sign of a band crossing. These properties fit in well with the study of Gross *et al.* [4] on identical bands in ^{77}Sr, ^{78}Sr, and ^{78}Rb, where the $[301]\frac{3}{2}$ orbital serves as a very good spectator. The present results would appear to confirm this interpretation.

V. CONCLUSIONS

A detailed in-beam study of the odd-odd nucleus ^{76}Rb has been carried out using the EUROGAM I γ-ray detector array in combination with the recoil separator at Daresbury. High-spin states in ^{76}Rb have been extended up to $I = (21^+)$ and (19^-). The hitherto unknown bandhead energy of the negative parity yrast band has been fixed and two new rotational bands have been identified and integrated into the level scheme. The three negative parity bands show very similar behavior, indicating similar configurations, and partly show rigid rotation. A $g_{\frac{9}{2}}$ proton crossing occurs in these bands at the frequency $\hbar\omega \approx 0.6$ MeV. Comparison with the ground state bands of ^{77}Rb and ^{77}Sr yields a striking resemblance in alignment and in the kinematical and dynamical moments of inertia, indicating that adding a proton or a neutron to the ^{76}Rb ground state configuration does not significantly affect the moment of inertia and deformation.

The alignment of both $g_{\frac{9}{2}}$ protons and neutrons is blocked in the positive parity bands. Instead a gradual alignment of the odd nucleons towards the rotational axis is observed. Agreement in both kinematical and dynamical moments of inertia as well as in alignment is found relative to a new band in ^{77}Rb, which is suggested to

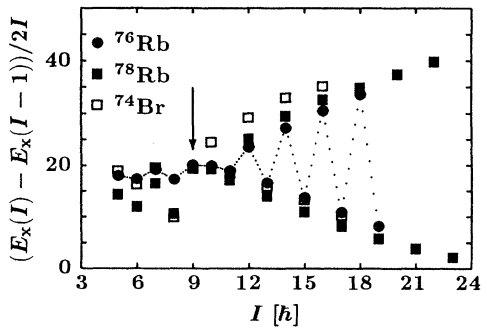

FIG. 6. Graphs of the quantity $[E_x(I) - E_x(I-1)]/2I$ as a function of I for the positive parity yrast bands in ^{76}Rb and ^{74}Br and the band built on the $I = 4$ isomer in ^{78}Rb. At $I = 9$ the phase of the alternating pattern reverses in all bands.

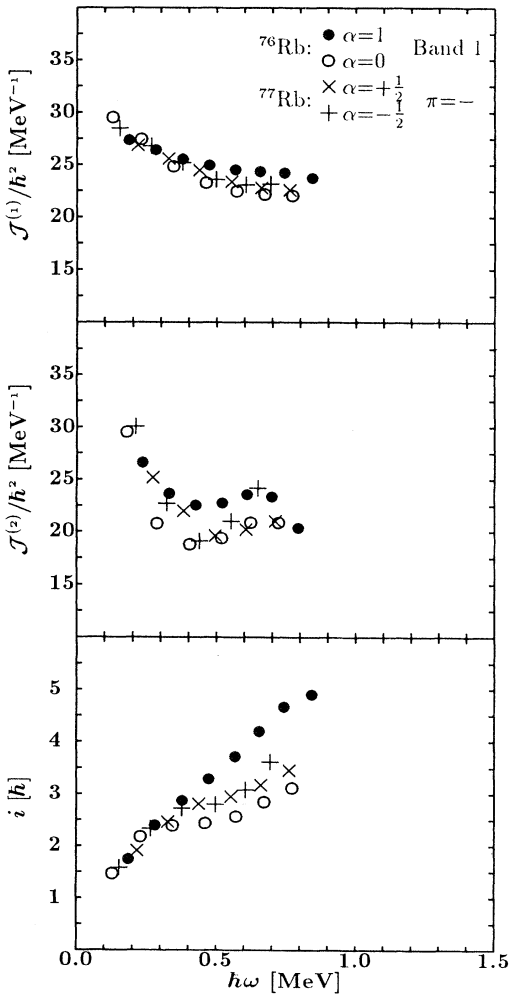

FIG. 7. Comparison of the kinematical ($\mathcal{J}^{(1)}$) and dynamical ($\mathcal{J}^{(2)}$) moments of inertia and the alignment i of band 1 in ^{76}Rb and a recently identified three-quasiparticle band in ^{77}Rb.

contain the same configuration with an additional neutron in the $[301]\frac{3}{2}$ Nilsson orbital. This fact confirms its proposed role as a very good spectator.

ACKNOWLEDGMENTS

The authors wish to thank C. Baktash, D. Sarantites, and the crew and staff of the Nuclear Structure Facility at Daresbury Laboratory for their assistance in this experiment. This work was funded in part by Deutsches Bundesministerium für Forschung und Technologie under Contract No. 06GÖ451, the Swedish Natural Science Research Council, and the U.S. Department of Energy under Contracts Nos. DE-FG02-88ER-40406, DE-FG02-91ER-40609, and DE-FG05-93ER40770. EUROGAM was funded by the UK Science and Engineering Research council and the Institute for Nuclear and Particle Physics, France.

[1] W. Nazarewicz, J. Dudek, R. Bengtsson, T. Bengtsson, and I. Ragnarsson, Nucl. Phys. **A435**, 397 (1985).
[2] L. Lühmann, K. P. Lieb, C. J. Lister, B. J. Varley, J. W. Olness, and H. G. Price, Europhys. Lett. **1**, 623 (1986).
[3] P. Lievens, L. Vermeeren, R. E. Silverans, E. Arnold, R. Neugart, K. Wendt, and F. Buchinger, Phys. Rev. C **46**, 797 (1992).
[4] C. J. Gross, C. Baktash, D. M. Cullen, R. A. Cunningham, J. D. Garrett, W. Gelletly, F. Hannachi, A. Harder, M. K. Kabadiyski, K. P. Lieb, C. J. Lister, W. Nazarewicz, H. A. Roth, D. Rudolph, D. G. Sarantites, J. A. Sheikh, J. Simpson, Ö. Skeppstedt, B. J. Varley, and D. D. Warner, Phys. Rev. C **49**, R580 (1994).
[5] H. Fischer, P. Dabkiewicz, P. Freilinger, H.-J. Kluge, H. Kremmling, R. Neugart, and E.-W. Otten, Z. Phys. A **284**, 3 (1978).
[6] D. M. Moltz, K. S. Toth, F. T. Avignone III, H. Noma, B. D. Kern, R. E. Tribble, and J. P. Sullivan, Nucl. Phys. **A427**, 317 (1984).
[7] R. B. Piercey, A. C. Rester, J. H. Hamilton, A. V. Ramayya, H. K. Carter, R. L. Robinson, H. J. Kim, J. C. Wells, and J. Lin, Phys. Rev. C **32**, 625 (1985).
[8] S. Hofmann, I. Zychor, F. P. Hessberger, and G. Münzenberg, Z. Phys. A **325**, 37 (1986).
[9] G. García-Bermúdez, C. Baktash, C. J. Lister, and M. A. Cardona, Phys. Rev. C **38**, 1083 (1988).
[10] J. H. McNeill, A. A. Chishti, W. Gelletly, B. J. Varley, H. G. Price, C. J. Lister, Ö. Skeppstedt, U. Lenz, C. J. Gross, J. Heese, and K. P. Lieb, *Manchester Nuclear Physics Report, Aug. 1987 - Dec. 1988*, edited by Schuster Laboratory, The University, Manchester, 1989, p. 27.
[11] C. W. Beausang, S. A. Forbes, P. Fallon, P. J. Nolan, P. J. Twin, J. N. Mo, J. C. Lisle, M. A. Bentley, J. Simpson, F. A. Beck, D. Curien, G. de France, G. Duchêne, and D. Popescu, Nucl. Instrum. Methods **313**, 37 (1992).
[12] P. J. Nolan, Nucl. Phys. **A520**, 657c (1990).
[13] F.A. Beck, Prog. Part. Nucl. Phys. **28**, 443 (1992).
[14] A. N. James, T. P. Morrison, K. L. Ying, K. A. Connell, H. G. Price, and J. Simpson, Nucl. Instrum. Methods A **267**, 144 (1988).
[15] M. K. Kabadiyski, K. P. Lieb, and D. Rudolph, Nucl. Phys. **A563**, 301 (1993).
[16] R. Bengtsson and S. Frauendorf, Nucl. Phys. **A327**, 139 (1979).
[17] C. J. Gross, J. Heese, K. P. Lieb, C. J. Lister, B. J. Varley, A. A. Chishti, J. H. McNeill, and W. Gelletly, Phys. Rev. C **39**, 1780 (1989).
[18] S. M. Harris, Phys. Rev. **138**, 509 B (1965).
[19] C. Ekström, S. Ingelman, G. Wannberg, M. Skarestad, and ISOLDE Collaboration, Nucl. Phys. **A311**, 269 (1978).
[20] C. J. Lister, B. J. Varley, H. G. Price, and J. W. Olness, Phys. Rev. Lett. **49**, 308 (1982).
[21] J. W. Holcomb, T. D. Johnson, P. W. Womble, P. D. Cottle, S. L. Tabor, F. E. Durham, and S. G. Buccino, Phys. Rev. C **43**, 470 (1991).
[22] A. J. Kreiner and M. A. J. Mariscotti, Phys. Rev. Lett. **43**, 1150 (1979).
[23] A. Harder, F. Dönau, M. K. Kabadiyski, K. P. Lieb, D. Rudolph, C. J. Gross, R. A. Cunningham, F. Hannachi, J. Simpson, D. D. Warner, H. A. Roth, Ö. Skeppstedt, and W. Gelletly (unpublished).